The influence of a dc electric field on chemical interactions in "peroxide-metal" systems during combustion processes

Sergey M. Busurin,[a] Maxim V. Kuznetsov,[a] Yury G. Morozov,[a] Mariya L. Busurina[a] and Ivan P. Parkin*[b]

Received (in Cambridge, UK) 20th October 2009, Accepted 17th December 2009
First published as an Advance Article on the web 19th January 2010
DOI: 10.1039/b9nj00579j

The influence of a dc-contactless electric field on the combustion of BaO_2–Fe and MnO_2–Fe systems was investigated. The degree of phase transformation during combustion was directly influenced by the external electric field. The mechanism of combustion in these systems, containing metal fuel and solid inner-reaction oxidizer, under conditions of an external electric field, are described. It was concluded that the field-promoted transport of active oxygen anions formed in the liquid phase of the heat-up zone of these combustion systems.

Alkaline and alkaline-earth metal peroxides have been successfully used in the combustion synthesis of complex oxide materials.[1–4] Metal peroxides are used for two purposes; firstly, for the maintenance of the combustion reaction due to oxygen release as a result of their decomposition, and secondly, to introduce the required chemical element into the crystal structure. At present, in the conventional synthesis of complex oxides, such reagents as oxides, carbonates or nitrites of barium and iron are used. Substitution of these components in the combustion reaction, for example BaO_2 for $BaCO_3$, allows an improvement in the "know-how" of powder production. It takes place due to the introduction of an additional inner-reaction source of oxygen. Also it enables the avoidance of nitrogen- and carbon-containing impurities in the synthesized products.

The combustion synthesis of barium hexaferrite under conditions of a dc electric field has been previously reported.[5] In this system, one of the green mixture components was barium peroxide. An external electric field (EEF) in a combustion process is the application of an external voltage across the system without inducing any direct heating effect. It has been shown[5–7] that the application of an EEF, E, during the combustion synthesis of ferrites leads to changes in the combustion process characteristics and product microstructure. This allows modification of the final product properties. It was also found that depending on the EEF intensity, crystalline materials with phase ratios corresponding to the primary desired ferritization product could be obtained. At "low" field values (starting from ZF), the main phase was $BaFe_{12}O_{19}$ up to E = 110 kV m^{-1}, whilst at larger fields, the Fe_2O_3 component was more prominent.[5] However, in these systems, the desired product was often detected in a complex mix of phases. This in turn did not allow identification of the separate stages at which the applied field affected the reaction. We suppose that such stages exist; for example: decomposition of the solid oxidizers, oxidation of the metal fuel (powder) and solid-phase interaction of the components behind the combustion wave front. In relation to uncovering the mechanism of the combustion process, a study of the influence of the EEF on two-component systems, containing only fuel and solid inner-reaction oxidizer, is reported here.

Here, we report the results of such an investigation of phase formation for reactions of manganese oxide or barium peroxide with iron metal under the influence of an EEF. Barium peroxide and iron metal are components of the system used to synthesize barium hexaferrite, $BaFe_{12}O_{19}$.[5] Due to the high exothermicity of this system, another similar system—BaO_2 + 2Fe (system I)—was chosen as the subject of the investigation reported here. The desired product of the reaction in this system is $BaFe_2O_4$. Also, for comparison, the influence of the EEF on the process and products of the interaction in a MnO_2 + 2Fe system (system II) were investigated with respect to the desired spinel manganese ferrite $MnFe_2O_4$.[6,7]

The combustion process in system I took place in a steady regime with the recorded maximum combustion temperature T_c = 1080 K and velocity U = 8 mm s^{-1}. The combustion wave was accompanied by a sparking bright orange gas flame. In Fig. 1, the X-ray diffraction patterns obtained from the combustion products of system I synthesized in a zero field (ZF) and in a dc EEF of E = 220 kV m^{-1} are presented. After synthesis in a ZF, the main phase present in the final product mixture was $BaFeO_{3-y}$. This material is representative of a family of compounds of variable oxygen content (y = 0–0.5). It includes $Ba_8Fe_8O_{21}$ (PDF 75-0427) and $Ba_2Fe_{30}O_{46}$ (PDF 73-2034), which were identified by Rietveld analysis (Table 1). The mutual superposition of reflections in the X-ray diffraction patterns explains in part the appreciable broadening of the main lines. In addition to the percentage of phase fractions identified above, $BaCO_3$ (PDF 41-0373) and Fe (PDF 03-1050) were also detected. The application of a 220 kV m^{-1} dc EEF during the combustion reaction increased the amount of $BaFeO_{3-y}$ phases identified ($Ba_8Fe_8O_{21}$ 40.8% and $Ba_2Fe_{30}O_{46}$ 14.6%, respectively). Accordingly, from the Rietveld analysis, the amounts of $BaCO_3$ and Fe were diminished to 29.6 and 15.2%, respectively.

Similar effects (Fig. 2) were also observed after analysis of the combustion products obtained under EEF conditions in

---

[a] *Institute of Structural Macrokinetics and Materials Science, Russian Academy of Sciences, 8 Institutskaya Street, Chernogolovka, Moscow Region, 142432, Russia*
[b] *Department of Chemistry, University College London, 20 Gordon Street, London, UK WC1H 0AJ. E-mail: i.p.parkin@ucl.ac.uk*

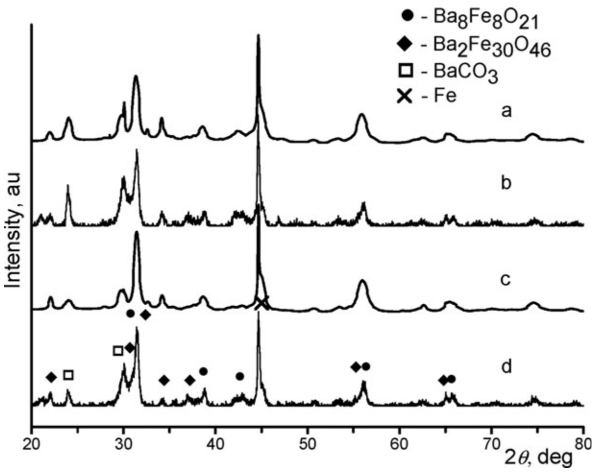

Fig. 1 X-Ray diffraction patterns of the combustion products in system I. DC applied EEF: (b) 0 and (d) +220 kV m^{-1}. (a) and (c): Graphic simulation analysis of the same patterns using the Powder Cell v.2.4 program and the ICSD database.

Table 1 Phase composition of the combustion products of system I

	$Ba_8Fe_8O_{21}$	$Ba_2Fe_{30}O_{46}$	$BaCO_3$	Fe
ZF	34.0	12.5	34.1	19.5
EEF	40.8	14.6	29.6	15.2

system II. In all of the combustion products made in ZFs, the main phase present was unreacted iron metal (PDF 01-1262). Besides that, Fe_3O_4 was also detected. After the application of an EEF (E = 220 kV m^{-1}), the X-ray diffraction patterns showed reflections belonging to the main lines of Fe_3O_4, and furthermore, the metallic iron content decreased two-fold (from 60% to ~25%). The measured combustion temperature under EEF conditions increased from its ZF value of 785 K to 845 K. Furthermore, the metastable phase $(Mn–Fe)_3O_4$, as well as more Mn_2O_3, was also found in the combustion products. It is necessary to note that in the combustion products obtained in ZFs, these phases were present in much smaller amounts. So, from the experimental results, the application of the EEF lead to an increase in the degree of phase transformation in both cases: BaO_2 + 2Fe (system I) and MnO_2 + 2Fe (system II).

Probable mechanisms of how the EEF influences these systems will now be discussed. Barium peroxide starts to desorb oxygen at ~770 K, with full decomposition being achieved at 1060 K.[8] This temperature corresponds approximately to the maximum combustion temperature observed in system I. However, the presence of metallic iron and its oxides in the system leads to changes in the properties of BaO_2. It is known[9] that metal oxides (in particular, Fe_2O_3) are catalysts of barium peroxide decomposition to the form BaO. The presence of Fe_2O_3 in the green mixture accelerates oxygen desorption processes from the barium peroxide at 770 K. This oxide operates as a catalyst to promote oxygen release from BaO_2. Above 870 K, Fe_2O_3 reacts with the nascent BaO because of its high chemical activity. As a result of these processes, the formation of the $BaFeO_{3-y}$ phase occurs as a layer growth at the interface between the oxides.

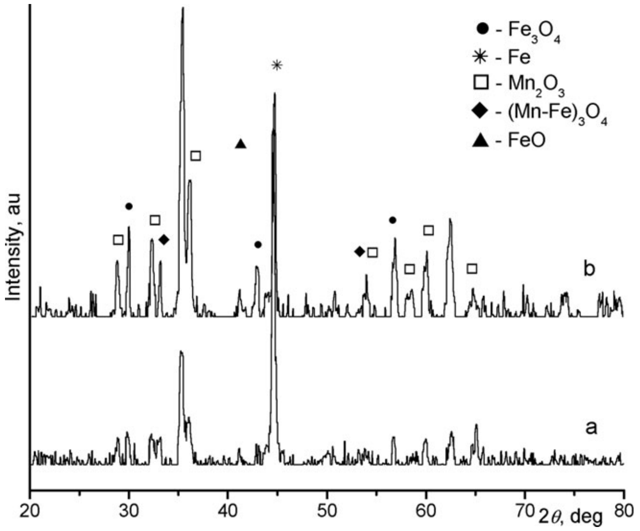

Fig. 2 X-Ray diffraction patterns of the combustion products in system II. DC applied EEF: (a) 0 and (b) +220 kV m^{-1}.

Microstructure studies of combustion products from system I (Fig. 3) showed that chemical interaction proceeds through a liquid phase in the combustion wave. It was seen that the application of an EEF lead to an increase of the desired phase fraction.

The change in phase fraction is related to the thermal decomposition of barium peroxide, which has a relatively complex character.

By using time resolved XRD (measuring sequential XRD patterns during heating), it has been previously shown that at 670 K, there is a dramatic decrease in the BaO_2 line intensity that is related to its fusion.[10] However, the BaO lines appeared only at 990 K.[10] When BaO_2 starts to lose active oxygen, the chemical equilibrium is displaced towards BaO formation. In the BaO_2 + 2Fe system, reactive oxygen (produced inside the reaction mixture) is spent on oxidation of the iron fuel. It is known[11] that an EEF accelerates the evaporation of polar liquids. With reference to our systems, the EEF promotes acceleration of the transport of active oxygen anions formed in the liquid phase of the heat-up zone. This leads to a shift of the equilibrium, according to the BaO_2–BaO[12] phase diagram, towards BaO formation. As a result of this, a higher proportion of BaO particles participate in the chemical reaction under applied EEF conditions. This mechanism is also supported by the fraction of $BaFeO_{3-y}$ compounds formed.

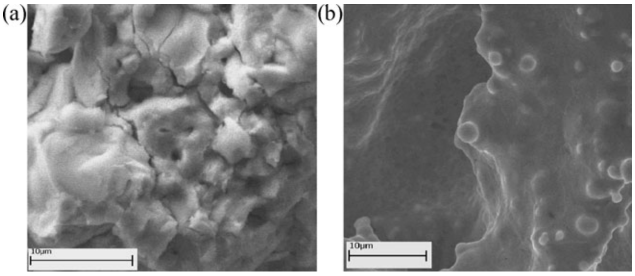

Fig. 3 Scanning electron microscopy (SEM) images of the combustion products in system I. DC applied EEF: (a) 0 and (b) +220 kV m^{-1}.

On the basis of all the data, it is possible to present the processes that took place during the combustion of system I in open air (carbon dioxide is one of air's components) as a set of equations:

$$BaO_2 \rightarrow BaO + 0.5O_2\uparrow \qquad (1)$$

$$3Fe + 2O_2 \rightarrow Fe_3O_4 \qquad (2)$$

$$Fe_3O_4 + 3BaO + O_2\downarrow \rightarrow 3BaFeO_{3-y} \qquad (3)$$

$$BaO + CO_2 \rightarrow BaCO_3 \qquad (4)$$

Here, it may be supposed that the EEF influences the degree of conversion of the processes described by eqns (1)–(4).

In Fig. 4, the TGA (Δm) and DTA (V) results obtained during the linear heating of the MnO_2 and MnO_2 + 2Fe (system II) are presented. We suppose that processes corresponding to the inflection seen in the MnO_2 + 2Fe heating process thermograms at 750 K could be attributed to the MnO_2 to Mn_2O_3 transformation. This process was accompanied by a mass loss and an endothermic effect. The presence of metallic iron lowers the onset temperature of MnO_2 decomposition because of its catalytic ability.[9] An endothermic effect at 763 K in the background of the common exothermic peak during iron oxidation testifies to this fact (Fig. 4). The mass starts to increase from the beginning of the exothermic oxidation reaction at 535 K and continues up to Mn_3O_4 formation at 1080 K. The increased quantity of Mn_2O_3 in samples prepared under EEF conditions may be related to the influence of the initial MnO_2 reduction on the process. It is known[13] that the application of an electrostatic field during the carbothermic reduction of some oxides essentially changes the reaction kinetics. The process characteristics include the degree of transition metal oxide reduction. A decrease in the starting temperature of the reduction process can also be observed. If we assume that under EEF conditions the degree of MnO_2 reduction (according to the XRD data) increases, then no change in the temperature of the reduction process should occur.

This was verified by thermograms of the combustion processes modelled in system II (Fig. 5). Application of the EEF slowed the temperature evolution of the reaction; the inflection point of the curve at 600 K was displaced in time (*ca.* 20 s *vs.* 12 s; Fig. 5). Furthermore, the maximum temperature reached was greater and accordingly an increase in the phase transformation was seen.

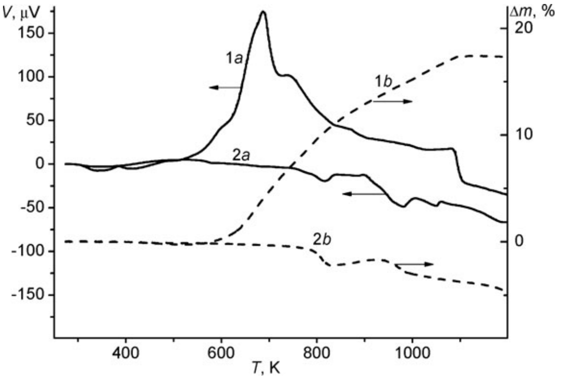

Fig. 4 (a) Solid lines: DTA results and (b) dashed lines: TGA results for the (1): MnO_2 + 2Fe system II and (2): the MnO_2 system, obtained under conditions of linear heating/cooling.

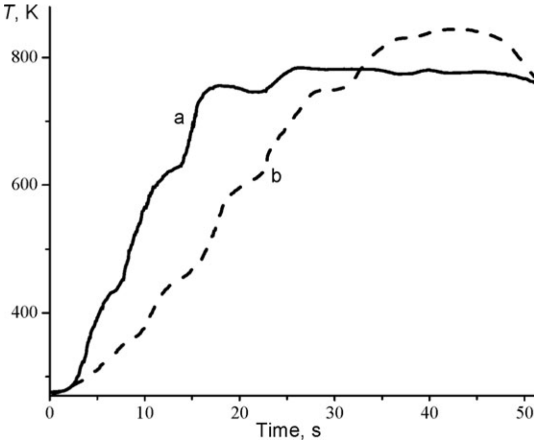

Fig. 5 Temperature profiles of the combustion processes in system II. DC applied EEF intensity: (a) 0 and (b) +220 kV m^{-1}.

In conclusion, the application of an EEF to combustion processes allows regulation of the phase formation and combustion regimes during chemical interactions in complex oxide systems. The mechanisms described for two different systems may be extrapolated to the other systems containing similar components. Investigating the influence of the EEF in such systems allows an increase in the degree of phase transformation during the combustion process, as well as facilitates the formation of products having the required chemical and morphological composition.

This work was supported by Russian Foundation for Basic Research grants RFBR nos. 07-08-00335-a and 10-08-01130-a, and a grant from the President of Russia MK-181.2009.8. I. P. P. thanks the Wolfson Trust/Royal Society for a merit award. I. P. P. and M. V. K. thank the Royal Society for a joint project grant.

Experimental

High purity powders of the green mixture, such as BaO_2 (d_{50} = 17.8 μm), MnO_2 (d_{50} = 14.0 μm) and Fe (d_{50} = 3.2 μm), were obtained from the Russian chemical market and used as supplied. The starting raw materials were mixed in a planetary ball mill for 10 min in appropriate steel bowls using steel balls whose mass was equal to half that of the raw material. The synthesis of samples of bulk density (mass = 15 g) was carried out in air in a quartz boat of size 50 × 30 × 15 mm. Combustion was initiated by means of a match without any additional initiating components (for example, Ti metal powder). Syntheses under EEF conditions were carried out according to a technique described previously.[5] The maximum EEF intensity was 220 kV m^{-1} (limited by apparatus and safety restrictions). During combustion, its front moved in the direction of the positively-charged voltage plate. Measurements of the combustion temperature and speed velocity were carried out by means of 200 μm chromel–alumel thermocouples. The phase and crystal structure of the combustion products were determined by X-ray diffraction analysis by means of a DRON-3.0 diffractometer (Cu-K$_\alpha$). X-Ray diffraction analysis data was processed using a Crystallographica

Search-Match (v.3.1.0.0) computer program and the Powder Diffraction File (PCPDFWIN v.2.02) database. The Powder Cell v.2.4 program was also used for Rietveld analysis. X-Ray profiles of lattices were calculated using the preferred orientation of the (000) plane within the 2D Rietveld–Toraya model. Background subtraction from the total powder pattern was represented as a seventh order polynomial. To describe the diffraction line profiles, a pseudo Voigt2 function was used that is a linear combination of Gaussian and Lorentzian. Microstructural research and elemental analyses were determined by a LEO 1450 Carl Zeiss scanning electron microscope with an INCA ENERGY 300 Oxford Instruments supplement for energy dispersive analysis. Thermogravimetric (TG) and differential thermal (DTA) measurements were carried out on TAG24S24 SETARAM equipment in a constant heating (cooling) regime in air with a 10 K min^{-1} rate up to 1273 K.

References

1 I. P. Parkin, M. V. Kuznetsov and Q. A. Pankhurst, *J. Mater. Chem.*, 1999, **9**, 273–281.
2 L. Affleck, M. D. Aguas, I. P. Parkin, Q. A. Pankhurst and M. V. Kuznetsov, *J. Mater. Chem.*, 2000, **10**, 1925–1932.
3 L. Affleck, M. D. Aguas, Q. A. Pankhurst, I. P. Parkin and V. A. Steer, *Adv. Mater.*, 2000, **12**, 1359–1362.
4 I. P. Parkin, G. Elwin, M. V. Kuznetsov, Q. A. Pankhurst, Q. T. Bui, G. D. Forster, L. Fernandez-Barquin, A. V. Komarov and Yu. G. Morozov, *J. Mater. Process. Technol.*, 2001, **110**, 239–243.
5 S. M. Busurin, Yu. G. Morozov, M. V. Kuznetsov, M. L. Chernega and A. A. Chobko, *Inorg. Mater.*, 2006, **42**, 1374–1378.
6 M. V. Kuznetsov, S. M. Busurin, Yu. G. Morozov and I. P. Parkin, *Phys. Chem. Chem. Phys.*, 2003, **5**, 2291–2296.
7 S. M. Busurin, Yu. G. Morozov, M. V. Kuznetsov, S. G. Bakhtamov and M. L. Chernega, *Combust., Explos. Shock Waves*, 2005, **41**, 421–425.
8 A. I. Efimov, L. P. Belorukova, I. V. Vasilkova and V. P. Chechev, *Properties of Inorganic Compounds*, Moscow, Khimiya, 1983, pp. 390.
9 I. I. Volnov, *Peroxide Compounds of Alkaline-Earth Metals*, Moscow, Nauka, 1983, pp. 136.
10 V. I. Ponomarev, A. G. Peresada, M. D. Nersesyan and A. G. Merzhanov, *Superconductivity: Physics, Chemistry, Technics*, 1990, **3**, 2813–2814.
11 N. N. Krasikov, *J. Tech. Phys.*, 2000, **70**, 120–121.
12 J. L. Jorda, T. K. Jondo and J. Alloys, *J. Alloys Compd.*, 2001, **327**, 167–177.
13 M. A. Vishkareva, V. V. Levina, D. I. Ryzhonkov and G. R. Umarov, *Izvestiya Vuzov. Ferrous Metallurgy*, 1996, **9**, 1–3.